RESEARCH ARTICLE

Malaria Induces Anemia through CD8$^+$ T Cell-Dependent Parasite Clearance and Erythrocyte Removal in the Spleen

Innocent Safeukui,[a,b] Noé D. Gomez,[a,c] Aanuoluwa A. Adelani,[a,b] Florence Burte,[d] Nathaniel K. Afolabi,[e] Rama Akondy,[f] Peter Velazquez,[g] Anthony Holder,[d] Rita Tewari,[h] Pierre Buffet,[i] Biobele J. Brown,[e] Wuraola A. Shokunbi,[j] David Olaleye,[k] Olugbemiro Sodeinde,[d,e] James Kazura,[l] Rafi Ahmed,[f] Narla Mohandas,[m] Delmiro Fernandez-Reyes,[d,e] Kasturi Haldar[a,b]

Boler-Parseghian Center for Rare and Neglected Diseases, University of Notre Dame, Notre Dame, Indiana, USA[a]; Department of Biological Sciences, University of Notre Dame, Notre Dame, Indiana, USA[b]; Feinberg School of Medicine, Department of Pathology, Northwestern University, Chicago, Illinois, USA[c]; Division of Parasitology, MRC National Institute for Medical Research, London, United Kingdom[d]; Department of Paediatrics, College of Medicine, University of Ibadan, University College Hospital, Ibadan, Oyo, Nigeria[e]; Emory Vaccine Center, Emory University School of Medicine, Atlanta, Georgia, USA[f]; Department of Microbiology and Immunology, Indiana University School of Medicine, South Bend, Indiana, USA[g]; Centre for Genetics and Genomics, School of Biology, University of Nottingham, Nottingham, United Kingdom[h]; INSERM-UPMC (Paris 6 University), Unité Mixte de Recherche s945, Paris, France[i]; Childhood Malaria Research Group, University College Hospital, Ibadan, Nigeria[j]; Department of Virology, College of Medicine, University of Ibadan, Ibadan, Nigeria[k]; Center for Global Health and Diseases, Case Western Reserve University, Cleveland, Ohio, USA[l]; Red Cell Physiology Laboratory, New York Blood Center, New York, New York, USA[m]

ABSTRACT **Severe malarial anemia (SMA) in semi-immune individuals eliminates both infected and uninfected erythrocytes and is a frequent fatal complication. It is proportional not to circulating parasitemia but total parasite mass (sequestered) in the organs. Thus, immune responses that clear parasites in organs may trigger changes leading to anemia. Here, we use an outbred-rat model where increasing parasite removal in the spleen escalated uninfected-erythrocyte removal. Splenic parasite clearance was associated with activated CD8$^+$ T cells, immunodepletion of which prevented parasite clearance. CD8$^+$ T cell repletion and concomitant reduction of the parasite load was associated with exacerbated (40 to 60%) hemoglobin loss and changes in properties of uninfected erythrocytes. Together, these data suggest that CD8$^+$ T cell-dependent parasite clearance causes erythrocyte removal in the spleen and thus anemia. In children infected with the human malaria parasite *Plasmodium falciparum*, elevation of parasite biomass (not the number of circulating parasites) increased the odds ratio for SMA by 3.5-fold (95% confidence intervals [CI$_{95\%}$], 1.8- to 7.5-fold). CD8$^+$ T cell expansion/activation independently increased the odds ratio by 2.4-fold (CI$_{95\%}$, 1.0- to 5.7-fold). Concomitant increases in both conferred a 7-fold (CI$_{95\%}$, 1.9- to 27.4-fold)-greater risk for SMA. Together, these data suggest that CD8$^+$-dependent parasite clearance may predispose individuals to uninfected-erythrocyte loss and SMA, thus informing severe disease diagnosis and strategies for vaccine development.**

IMPORTANCE **Malaria is a major global health problem. Severe malaria anemia (SMA) is a complex disease associated with partial immunity. Rapid hemoglobin reductions of 20 to 50% are commonly observed and must be rescued by transfusion (which can carry a risk of HIV acquisition). The causes and risk factors of SMA remain poorly understood. Recent studies suggest that SMA is linked to parasite biomass sequestered in organs. This led us to investigate whether immune mechanisms that clear parasites in organs trigger anemia. In rats, erythropoiesis is largely restricted to the bone marrow, and critical aspects of the spleen expected to be important in anemia are similar to those in humans. Therefore, using a rat model, we show that severe anemia is caused through CD8$^+$ T cell-dependent parasite clearance and erythrocyte removal in the spleen. CD8 activation may also be a new risk factor for SMA in African children.**

Received 13 December 2014 **Accepted** 16 December 2014 **Published** 20 January 2015

Citation Safeukui I, Gomez ND, Adelani AA, Burte F, Afolabi NK, Akondy R, Velazquez P, Holder A, Tewari R, Buffet P, Brown BJ, Shokunbi WA, Olaleye D, Sodeinde O, Kazura J, Ahmed R, Mohandas N, Fernandez-Reyes D, Haldar K. 2015. Malaria induces anemia through CD8$^+$ T cell-dependent parasite clearance and erythrocyte removal in the spleen. mBio 6(1):e02493-14. doi:10.1128/mBio.02493-14.

Editor John C. Boothroyd, Stanford University

Address correspondence to Kasturi Haldar, khaldar@nd.edu.

This article is a direct contribution from a Fellow of the American Academy of Microbiology.

Malaria continues to be a major health challenge in the world. *Plasmodium falciparum* causes the most virulent form of human malaria. In 2012, it killed over 600,000 children, largely in sub-Saharan Africa (1). The asexual-blood-stage parasite infects erythrocytes and is responsible for all of the symptoms and pathology associated with disease. Uncomplicated malaria consists of cycles of high fever and chills. Severe malaria includes additional pathologies, including anemia, respiratory distress, lactic acidosis, and cerebral malaria (2).

Severe malaria greatly increases the risk of death. The major pathophysiological state is severe malarial anemia (SMA). SMA is a complex disease, associated with partial immunity and results from the loss of both uninfected and infected erythrocytes, along with a concomitant block in erythropoiesis (2–4). Rapid hemo-

globin reductions of 20 to 50% are commonly observed (5) and must be rescued by transfusion (which can carry a risk of other infections). However, the cause of this reduction and whether it also inexplicably influences dyserythropoiesis remain poorly understood. SMA in human populations is not proportional to circulating parasitemia, and recent studies suggest that it is linked to total parasite biomass sequestered in organs (6, 7). This led us to query whether immune mechanisms that kill parasites in organs may trigger anemia.

Mechanistic investigation can be greatly facilitated by relevant animal models and organ systems with physiological correspondence to human systems. Malarial anemia has previously been investigated in several mice and rat models (8–11). Murine models are attractive due to the availability of genetics and related tools. However, one drawback is that erythropoiesis, which in humans is in the bone marrow, is anomalously active in the mouse spleen (especially in response to a stress like anemia) (9, 12). This profoundly influences the organizational and functional components of an organ expected to be important in erythrocyte removal, a major mechanism of anemia (9). In contrast, in rats, erythropoiesis is largely restricted to the bone marrow, and critical aspects of the spleen red pulp architecture are similar to those of humans (13, 14). Hence, the pathophysiology of human splenic disease is likely to be better mimicked and measured in rats, whose larger size also facilitates monitoring anemia. Here, we have utilized the Wistar rat model, where malarial anemia is due to erythrocyte removal rather than dyserythropoiesis (8). We elucidate splenic mechanisms that exacerbate anemia by erythrocyte removal (up to ~50 to 60% hemoglobin reduction). We further extend these findings to patient studies and thus identify new risk factors for SMA in African children.

RESULTS

Comparative analysis of spleens and livers from aged Wistar rats infected with *Plasmodium berghei* ANKA reveals that the spleen shows mass expansion associated with anemia and the major parasite burden.

Rats infected with wild-type *P. berghei* ANKA displayed low peripheral parasitemia (3%) that peaked at day 8 postinfection (p.i.) (Fig. 1A). At day 10, peripheral parasitemia and the hematocrit declined. By days 12 to 14, parasites were completely eliminated, with an ~20% reduction in the hematocrit (range, 16 to 40%), suggesting simultaneous clearance of both infected and uninfected erythrocytes (the variation in hematocrit reduction is characteristic of an outbred model [8, 10]). The subsequent robust increase of reticulocytes (Fig. 1B) confirmed that erythrocyte reduction (or anemia) was not due to a block in erythropoiesis. Rather, it was by removal of uninfected erythrocytes (since the hematocrit declined 20% at 3% parasitemia). After recovery from anemia (days 24 to 28), the animals were cured and immune to subsequent parasite challenge (8, 10).

Since this is a model of malarial anemia, the spleen and the liver are expected to be the major affected organs. Notably, there was, on average, a >5-fold increase in spleen mass but no increase in liver mass by day 10 (Fig. 1C). Elevation of mean corpuscular volume (MCV) and mean corpuscular hemoglobin (MCH), highly characteristic of stress erythropoiesis, in the bone marrow (as in humans) was also noted (Fig. 1D and E), suggesting that the splenic expansion shown in Fig. 1C was not linked to increased splenic erythropoiesis (as in murine systems) but that it may play a major role in the removal of infected and uninfected erythrocytes.

Anemia has been linked to total parasite biomass in organs in human *falciparum* malaria (7). Quantitative PCR (qPCR) revealed that at day 8 (of peak infection), the rat spleen was the major site of *P. berghei* burden, containing over 70% of the parasites (Fig. 1F, upper panel). By day 10, there was a 34-fold reduction in the number of parasites in the spleen (to levels lower than in the liver, which remained unchanged), and the dynamics of splenic clearance was the same for wild-type and mutant parasites (10). Pathological analyses of lung, kidney, and brain failed to reveal significant parasite material compared to that in the spleen or even the liver (see Fig. S1 in the supplemental material). The lung showed small mass fluctuations, but they were largely reductions, and their dynamics were not coincident with peak infection, numbers of detectable parasites, or anemia (see Table S1). Together, these data suggested that spleen was the major site of parasite burden. Moreover, the timing of parasite elimination was also that of erythrocyte clearance and anemia.

We further investigated a *P. berghei* ANKA mutant with a deletion of *msp7*, a gene implicated in blood cell invasion and thus likely to influence total parasite load and anemia (10). At day 8, there was no difference in parasite loads in the liver, but in the spleen, the Δ*msp7* strain's peak load was 3-fold lower than that of its wild-type counterpart (Fig. 1F). Δ*msp7* strain clearance was coincident with a 14-fold reduction in spleen parasites at day 10 and a 10% reduction of uninfected erythrocytes at day 12 (Fig. 1F). This comparative analysis of the Δ*msp7* and wild-type parasites suggested that increasing fold parasite clearance in the spleen escalated uninfected-erythrocyte removal and thus anemia.

Expansion of splenic CD8$^+$ T cells, in wild type relative to Δ*msp7* infection. To understand in an unbiased way splenic processes that underlie increased clearance of parasite load (rather than overall infection *per se*), we examined differences in host response to wild-type parasites relative to Δ*msp7* mutant parasites. To do this, we undertook whole-genome microarray expression analyses of wild-type- relative to mutant-infected spleens at day 10 (uninfected animals were also included as controls) (Fig. S2A). Three hundred seventy-seven genes showed significant changes in expression (>1.5-fold change, $P = 0.005$) (Table S2A). In the top network (Fig. 2A), 7 (of the top 20) genes were for granzymes (including granzyme B), suggesting involvement of CD8$^+$ T cells or NK cells.

Flow cytometry analyses confirmed that *P. berghei* infection induced infiltration of B cells, NK cells, and CD3$^+$ T cells (both CD8$^+$ and CD4$^+$ T cells) in the spleen (see the combined information of Fig. 2B and C and S2B and C). NK cell counts remained low, with no difference seen between wild-type- and mutant-infected spleens (Fig. 2B), which also showed no significant differences in B cell counts (Fig. S2B). Wild-type-associated elevation was seen in CD3$^+$ T cells, with a 1.5-fold increase in CD8$^+$ T cells on day 10 in wild-type- compared to Δ*msp7* mutant-infected cells (Fig. 2C).

Quantitative immunohistochemical (IHC) analyses of spleen zones revealed that compared to Δ*msp7* mutant-infected animals, wild-type-infected animals showed specific, 2-fold increases in CD8$^+$ T cell concentrations in the white pulp/periarteriolar lymphoid sheaths and marginal zone (WP/PALS and MZ) at day 8 (Fig. 2D). By day 10, the CD8$^+$ T cells had migrated to the red pulp (RP) (Fig. 2D and S2C and D). The 2-fold increase in specific

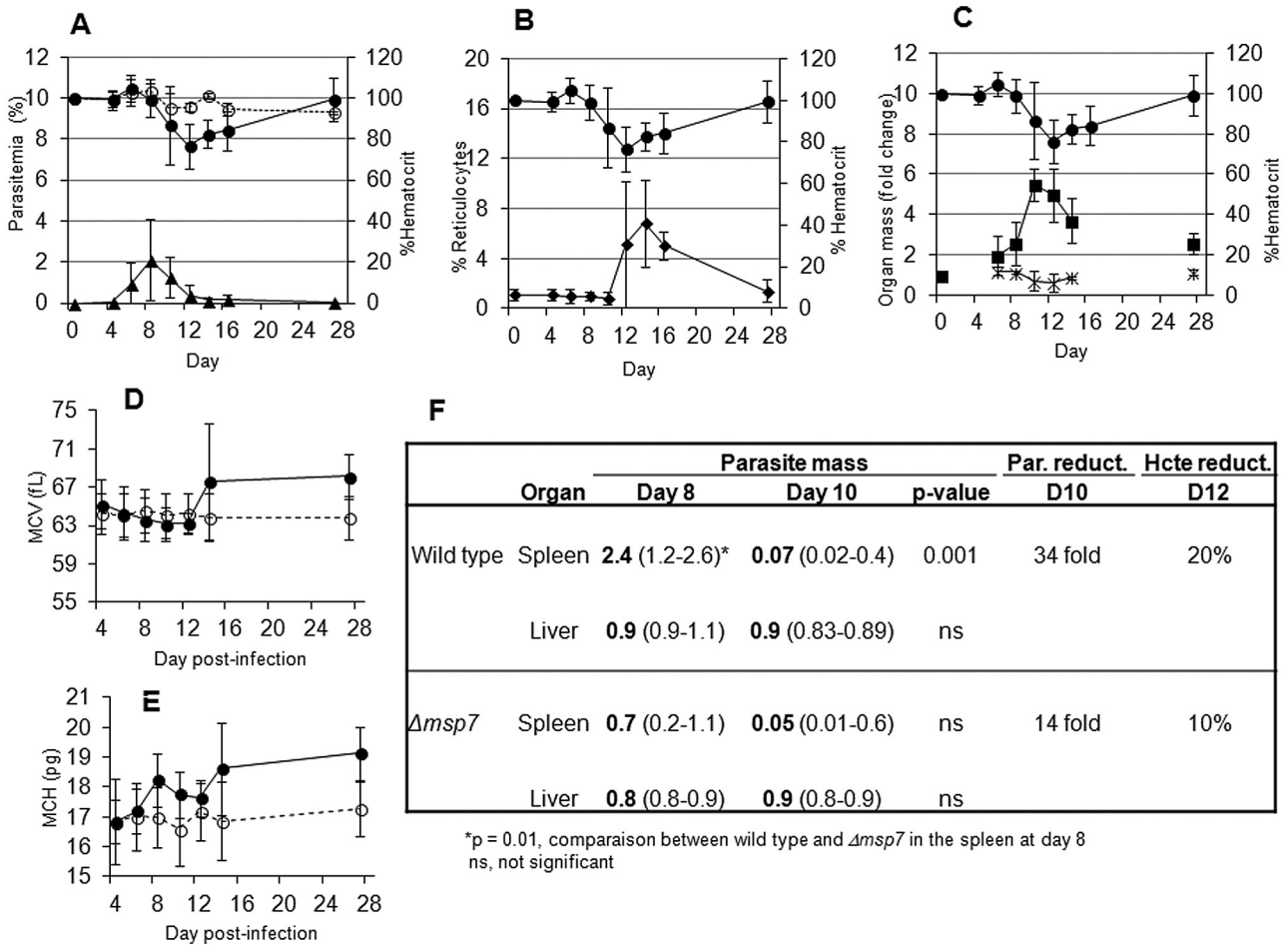

F

	Organ	Parasite mass Day 8	Parasite mass Day 10	p-value	Par. reduct. D10	Hcte reduct. D12
Wild type	Spleen	**2.4** (1.2-2.6)*	**0.07** (0.02-0.4)	0.001	34 fold	20%
	Liver	**0.9** (0.9-1.1)	**0.9** (0.83-0.89)	ns		
Δmsp7	Spleen	**0.7** (0.2-1.1)	**0.05** (0.01-0.6)	ns	14 fold	10%
	Liver	**0.8** (0.8-0.9)	**0.9** (0.8-0.9)	ns		

*p = 0.01, comparaison between wild type and *Δmsp7* in the spleen at day 8
ns, not significant

FIG 1 In aged Wistar rats, the spleen is the major site of parasite burden and clearance. (A to E) Malarial anemia induced by *P. berghei* ANKA in aged Wistar rats. (A to C) Anemia (filled circles) is measured as a reduction in hematocrit (right-panel *y* axis scale). (A) Dynamics of peripheral parasitemias in infected rats (filled triangles) and hematocrits in uninfected rats (open circles); (B) reticulocytosis (filled diamonds) and hematocrits (filled circles); (C) mass change in spleens (filled squares) and livers (multiplication signs). Dynamics of mean corpuscular volume (MCV) (D) and mean corpuscular hemoglobin (MCH) (E) are also shown for infected (filled circles) and uninfected (open circles) rats. (F) Comparative analysis of relative parasite mass and its change in the spleen and liver, correlated with anemia. Ratios of spleen and liver parasite loads were established by qPCR from rats infected with wild-type or Δ*msp7* parasites at (i) the peak of infection on day 8 and (ii) parasite reduction (Par. reduct.) day 10 (D10), suggesting 3- to 4-fold-higher levels of wild-type than of mutant parasites in the spleen on day 8; in contrast, the day 8 peak peripheral parasitemia of the wild-type parasites was 3%, compared to 2% for Δ*msp7* mutant parasites, but the dynamics were unchanged (10; data not shown). Maximal hematocrit reduction (Hcte reduct.), i.e., peak anemia, was measured at day 12. The time point selection in panel F was based on time points in panels A to C, and the time course of peak infection and anemia induced by the Δ*msp7* mutant was identical to that seen with wild-type parasites (10). The fold spleen parasite clearance and percent hematocrit reduction were ~2-fold higher in rats infected with the wild type (34-fold, 20%) than in rats infected with the Δ*msp7* mutant (14-fold, 10%). For panels A to E, the mean values and standard deviations are as shown. The data presented are representative and are from one out of two independent experiments with 3 to 4 animals in each group and for each time point. For the mean comparisons in panel F, one-way ANOVA with a Tukey *post hoc* analysis was used.

splenic zones detected by IHC analysis corresponded well to the 1.5-fold increase detected in the whole spleen by flow cytometry. IHC analysis showed no statistically significant differences in numbers of $CD4^+$ T cells or macrophages (Fig. S3). Although wild-type infections showed modest increases in $CD8^+$ and $CD4^+$ T cells in the liver (Fig. S4), the absolute number of $CD8^+$ and $CD4^+$ T cells in the spleen were 8- to 10-fold higher than in the liver (Table S3). Numbers of $CD68^+$ cells were also increased in spleen (Table S3).

Together, these data revealed that in wild-type relative to Δ*msp7* mutant infection, the major immune cell differences were in the spleen. Moreover, at day 10, the onset of parasite clearance, there was elevation in the number of $CD8^+$ T cells in the spleen RP (where parasites are eliminated), suggesting that $CD8^+$ T cells may be linked to blood-stage parasite clearance.

Requirement of $CD8^+$ T cells: effects on parasite control and anemia. The requirement for $CD8^+$ T cells in controlling blood-stage infection was tested in rats injected with anti-CD8α (Fig. 3A), which led to depletion of >95% of $CD8^+$ T cells (Fig. 3B, left side). Levels of $CD4^+$ T cells (Fig. 3B, right panel) and other immune cells (Fig. S5A and B) were unaffected. $CD8^+$ T cell depletion had no significant effect on the rise in parasitemia or peak parasitemia. It blocked subsequent reduction of parasitemia (Fig. 3C), sustaining it through day 10 to 12, when parasites are usually eliminated. A time course of $CD8^+$ T cell repletion suggests high-level restoration on day 15 and later (Fig. 3D). Immu-

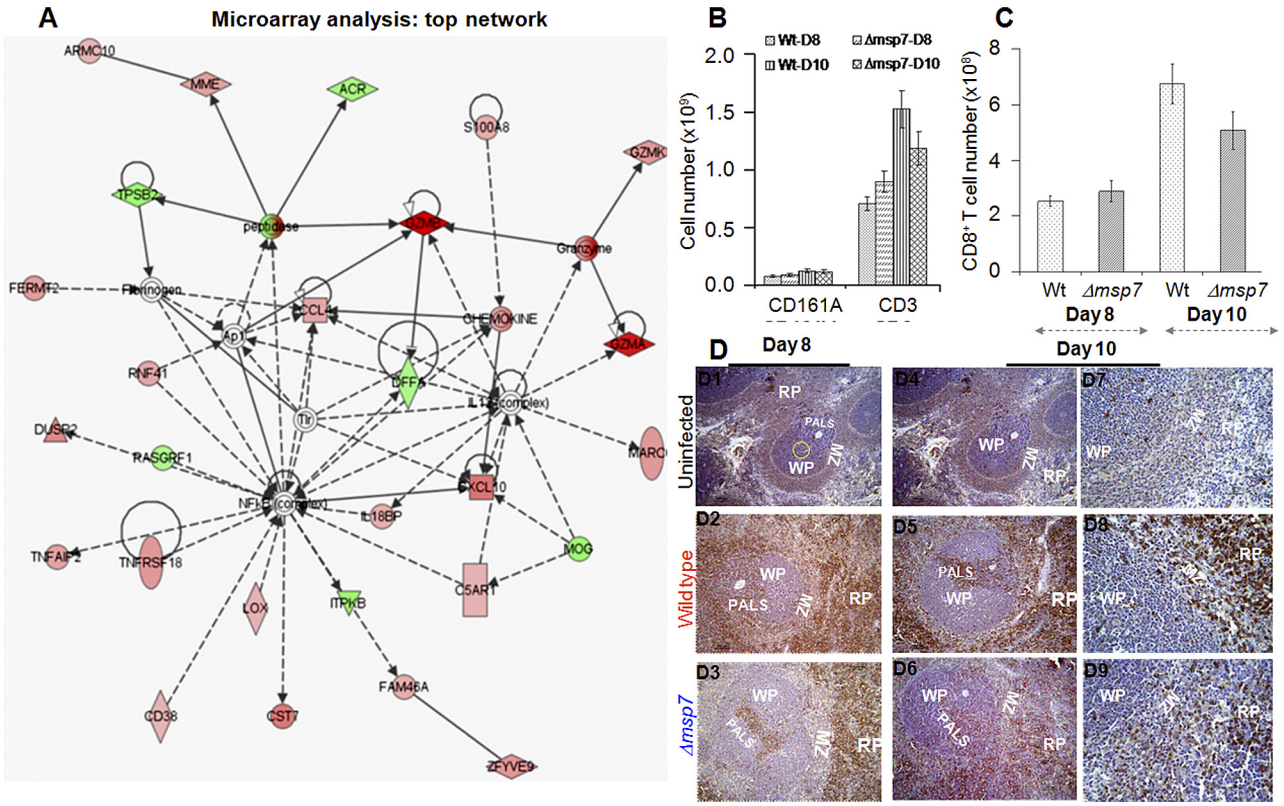

FIG 2 Expansion of CD8$^+$ T cells in the rat spleens upon infection with wild-type relative to Δ*msp7* parasites. (A) Inflammatory and immunological disease pathways predicted by ingenuity pathway analysis (IPA) of gene expression induced by wild-type relative to Δ*msp7* parasites on day 10. Red, highly upregulated genes (such as those for the granzymes GZM A and B); pink, genes with moderately increased expression (GZM K, CXCL10, CCL4 S100, and other inflammatory markers); green, downregulated genes. A full list of rat gene transcripts elevated in rats infected with wild-type relative to mutant parasites is shown in Table S2. (B and C) Flow cytometric analysis of NK cells (CD161A) and CD3$^+$ T and CD8$^+$ T cells from spleens of animals infected with wild-type (Wt) or Δ*msp7* mutant parasites at day 8 (D8) and day 10 (D10) p.i. (D) Immunohistochemical staining of CD8$^+$ T cells in the spleens of uninfected and wild-type- or Δ*msp7* parasite-infected rats at day 8 or 10 p.i. The CD8$^+$ T cell density was significantly higher in infected than in uninfected animals (although very low levels of CD8$^+$ T cells are seen in uninfected spleens [see the yellow circle in panel D1, which is magnified further in Fig. S2C]). Quantitative analysis (results are shown in Fig. S2D) confirmed that wild-type infection resulted in higher numbers of CD8$^+$ T cells than Δ*msp7* mutant infection. In addition, in wild-type-parasite infections, CD8$^+$ T cells were more highly concentrated in the white pulp (WP) or marginal zone (MZ) on day 8 and in the red pulp (RP) on day 10. PALS, periarteriolar lymphoid sheath. Original magnifications, ×100 (D1 to -6), ×400 (D7 to -9).

nohistochemical analysis at day 10 revealed that anti-CD8α resulted in a 2- to 3-fold reduction of splenic CD8$^+$ T cells (Fig. 3E and F), with no effect on dendritic cells (see also Fig. S5C and D), and in an elevation of splenic parasites (Fig. 3G). Repletion in CD8 T cells and the associated parasite clearance resulted in a deeper anemia (40% hemoglobin loss) (Fig. 3H).

Neither parasites alone (days 0 to 5) nor CD8$^+$ T cells alone (days 18 to 22) induced anemia. Both were detected from days 6 to 16, and during the adaptive phase (days 10 to 14), parasite clearance mediated by CD8$^+$ T cells was associated with severe anemia (Fig. 3H). The anemia was followed with a significant increase in the number of reticulocytes in the peripheral circulation (Fig. 3I), with characteristics of bone marrow-associated erythropoiesis (Fig. S5E to H). Moreover, since the peak parasitemias achieved were ~3%, 40 to 60% anemia was principally due to removal of uninfected red blood cells, as expected in this model. Analysis of the dynamics in individual animals (showing interanimal variability in outbred species) further confirmed the association between the requirement of parasitemia and CD8$^+$ T cells and anemia (Fig. S6). Together, these data suggest that CD8$^+$ T cells regulate the clearance of parasites, which in turn induces anemia.

Activation of CD8$^+$ T cells in the spleen is proportional to parasite load in the organ and soluble CD8 (sCD8) in plasma. Because CD8$^+$ T cells regulate parasite clearance, day 10 is the onset of clearance, and the RP is a major site (15), we investigated the activation of CD8$^+$ T cells at this time point in the spleen. Unfortunately, there are only a limited number of well-developed markers for cellular analysis in rats. As an alternative, we used microarray data that yielded extensive, genome-wide activation readouts and compared them to transcriptional signatures characteristic of murine CD8$^+$ T cell activation elicited by viral and bacterial infections (16). These analyses revealed expression patterns typical of effector CD8$^+$ T cells (downregulation of the interleukin 7 receptor [IL-7R] and Bcl-2 and upregulation of E2Fs) in splenocytes infected with the wild type and mutant compared to their uninfected counterparts (Fig. 4A; Table S2B). Further, among the differentially expressed genes in rats infected with the wild type versus the mutant, there are several (such as the granzyme genes) in common with those identified in murine effector CD8$^+$ T cells (Fig. 4A).

Numbers of activated splenic CD8$^+$ T cells were proportional to parasite load in the organ (Fig. 4B). We also examined sCD8,

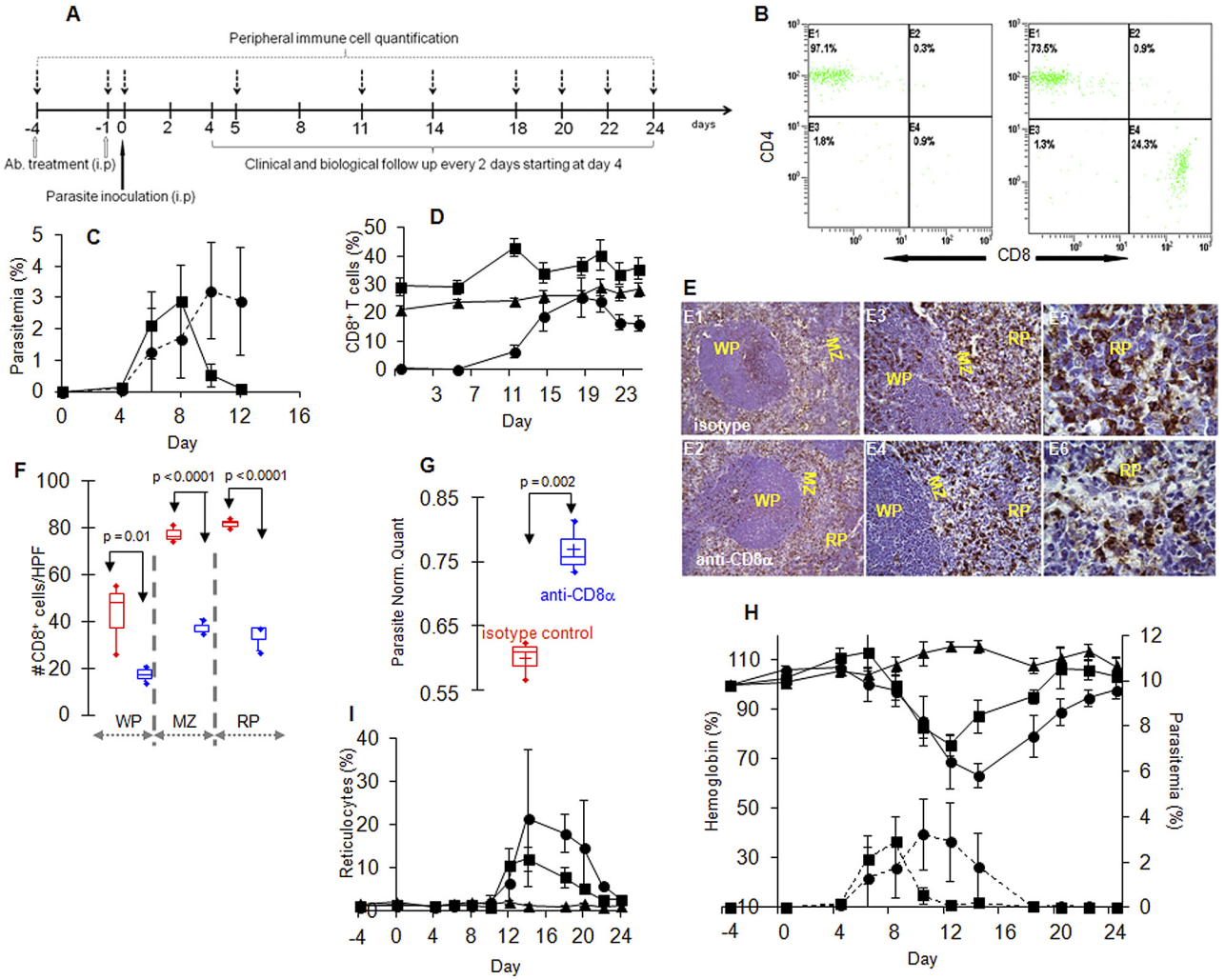

FIG 3 Effect of CD8$^+$ T cell depletion on parasitemia, the reticulocyte response, and anemia. (A) Experimental timeline of immunodepletion of CD8$^+$ T cells, time of antibody and parasite injection, and sampling of immune cells and other indicated parameters over 28 days (see also Materials and Methods). (B) Flow cytometry analysis at day 0, confirmed depletion of peripheral CD8$^+$ T cells in animals treated with anti-CD8α (left side) compared to isotype control Ab (right side). PBMCs were also stained for CD4, CD3, and B (CD45RA) markers and analyzed by flow cytometry. (C) Depletion of CD8$^+$ T cells showed no effect on the rise of parasitemia, but on day 12, when parasites were eliminated in isotype controls (filled squares), they remained at peak values in depleted animals (filled circles). (D) Dynamics of peripheral CD8$^+$ T cells (expressed as a fraction of total CD3$^+$ T cells) in animals treated with anti-rat CD8α (filled circles) or isotype control antibodies (filled squares), as well as in untreated (filled triangles) animals. Infected animals have higher levels of CD8$^+$ T cells than uninfected animals. However, after anti-CD8α treatment, CD8$^+$ T cell levels remained undetectable for 5 days in infected animals. From days 5 to 18, they rose and reached state levels. (E) Distribution of CD8$^+$ T cells (stained brown) in the spleens of isotype control and immunodepleted animals on day 10 as detected by IHC analysis. (F) Quantification of CD8$^+$ T cells in panel E. (G) Parasite loads in the spleens (detected by qPCR) of immunodepleted animals are higher than in isotype controls on day 10. Norm. Quant, normal quantity. (H) Induction of anemia (unbroken lines) as measured by the percent hemoglobin reduction (left-side *y* axis) in animals treated with anti-rat CD8α (filled circles) and isotype control antibodies (filled squares), as well as in untreated (filled triangles) animals. Associated peripheral parasitemias (right-side *y* axis) and their clearance are shown with dashed lines. (I) The reticulocyte response was increased in animals treated with anti-CD8α Ab (filled circles) compared to that in animals treated with the isotype control (filled squares). Mean values and standard deviations are shown in panels C, D, H, and I. The data are representative of one experiment of three independent experiments that contained 5 to 6 animals in each treatment group. For the mean comparisons, one-way ANOVA with a Tukey *post hoc* analysis (F) and Student's *t* test (G) were used.

because it is a form of the receptor released after activation (17, 18). sCD8 has been reported to be derived from CD4$^+$ T cells in certain circumstances of viral infection, autoimmunity, and transplantation (19). However, in our model, the CD4$^+$ T cell response is not altered between wild-type and *msp7* mutant infections (Fig. S2) and CD4$^+$ T cell numbers were not reduced when rats were perfused with anti-CD8α that immunodepleted CD8$^+$ T cells (Fig. 3 and S5A), suggesting that the CD4$^+$ CD8$^+$ T cell subpopulation is not induced in malarial infection. Indeed, we find that plasma sCD8 levels strongly and positively correlated with CD8$^+$ T cell number (Fig. 4C) (Spearman $r = 0.9$, $P < 0.0001$) and parasite load (Fig. 4D) (Spearman $r = 0.8$, $P = 0.20$).

Activated CD8$^+$ T cells are known to directly kill intracellular pathogens (20–22). This requires antigen presentation by the major histocompatibility complex (MHC) class I, which we detected on both uninfected and infected reticulocytes as well as white cells (Fig. 4E). We further detected specific production of gamma interferon (IFN-γ) by CD8$^+$ T cells stimulated with infected reticu-

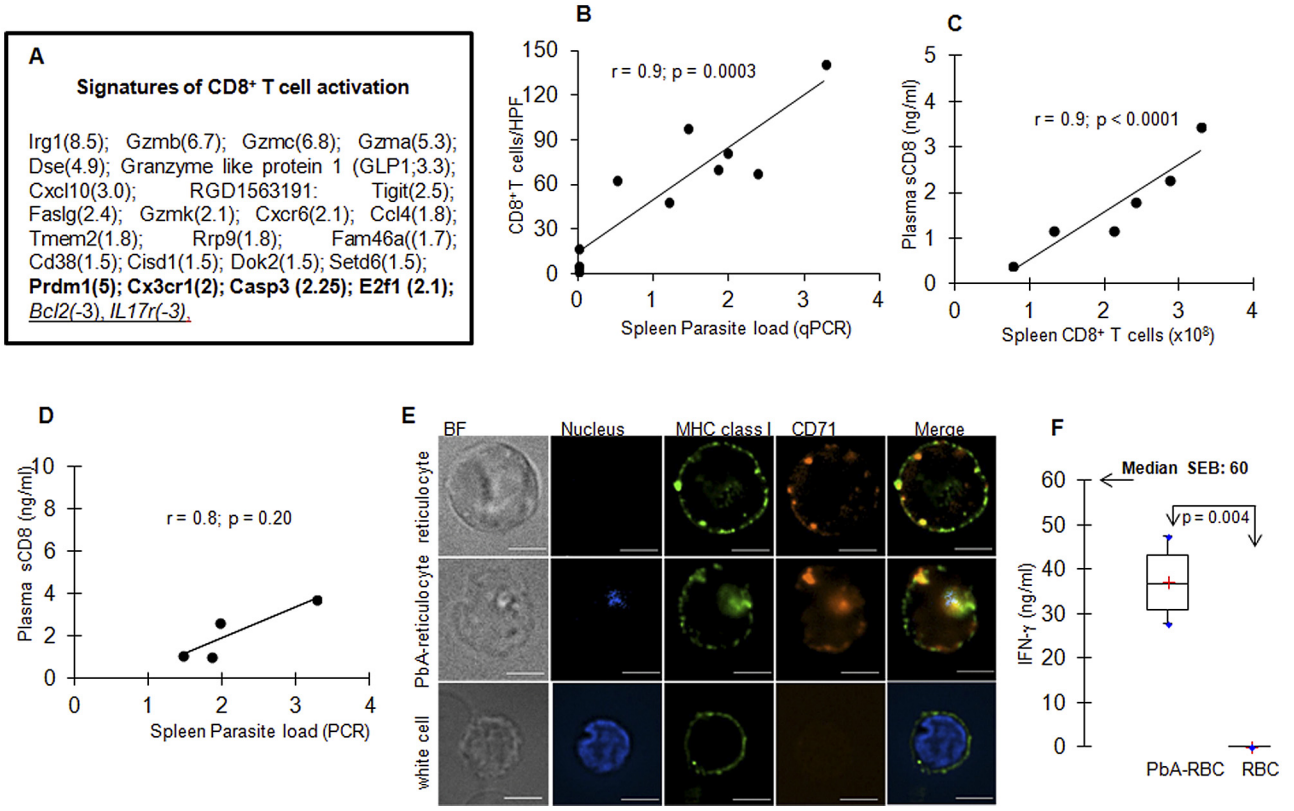

FIG 4 Activation of splenic CD8$^+$ T cells, which is proportional to the parasite load in the organ and sCD8 released into the plasma. (A) Rat gene transcripts that are elevated in wild-type-parasite relative to Δ*msp7* mutant infections (Table S2A) and also found in murine CD8$^+$ T cell activation (16). Fold change is shown in parenthesis. In bold are additional genes typical of effector CD8$^+$ T cells seen in wild-type-parasite- and mutant-parasite-infected splenocytes relative to their uninfected counterparts (see also Table S2B). Italicized, underlined genes are downregulated. (B) Quantification of CD8$^+$ T cells (detected by immunohistochemistry) indicates that they are directly proportion to parasite load (detected by qPCR) in the spleen. (C) Plasma levels of sCD8 (detected by ELISA) are directly proportional to CD8$^+$ T cell numbers quantified in the spleen. (D) Plasma levels of sCD8 are directly proportional to parasite load in the spleen. The Spearman correlation coefficient was used to determine the correlation shown in panels B to D. (E) Detection of MHC class I on uninfected and infected reticulocytes. Blood specimens from infected animals were labeled with the indicated primary antibodies directly conjugated to fluorescent chromophores in live-cell assays (see also Materials and Methods) to detect CD71 (a transferrin receptor, a marker for reticulocytes [red]), MHC class I (green), and DAPI (to label parasite or host nuclei [blue]) and viewed by Delta vision deconvolution microscopy. Marker distribution detected on uninfected and *P. berghei*-infected reticulocytes and a white cell are shown. (F) *In vitro* stimulation of day 10, CD8$^+$ T cells by *P. berghei*-infected erythrocytes taken from the same animals (see also Materials and Methods), measured by IFN-γ production. Median values of IFN-γ production by bacterial SEB antigen (positive control) are shown. Student's *t* test was used for the mean comparisons. PbA, *P. berghei* ANKA; RBC, red blood cells.

locytes *in vitro* (Fig. 4F), although the number of CD8$^+$ T cells and infected cells were limiting because they were from the same animal (since this is an outbred model). Although we show that CD8$^+$ T cells are (i) activated in response to blood-stage infection *in vitro* and (ii) control parasitemia *in vivo*, the lack of information on MHC class I presentation in this outbred rat model precludes establishing whether activation is indirectly or directly stimulated by infected erythrocytes.

Changes in properties of uninfected erythrocytes in malarial anemia. Under physiological conditions, the spleen is the major site of clearance of (aged and altered) erythrocytes. Since splenic clearance mechanisms detect changes in cellular properties of erythrocytes, we examined peripheral erythrocytes from infected rats on discontinuous Percoll gradients (Fig. 5A and B). On these gradients, infected erythrocytes (asterisk in Fig. 5A) and reticulocytes (Fig. 5A) were detected in the top light fraction (48%), while uninfected erythrocytes were detected at intermediate and higher densities (50% and greater). Visual representation and cell counts of various density fractions on different days suggested that infection increases the relative density of uninfected erythrocytes. As shown in Fig. 5B, at day 12 (a time of active erythrocyte removal), uninfected erythrocytes from all three infected animals consistently showed higher density fractions at 54%, 58%, and 60% Percoll, accounting for 20 to 40% of erythrocytes, which well corresponds to the extent of erythrocyte removal seen in this animal model. Since the spleen also has high concentrations of erythrocytes, we propose a splenic model for erythrocyte clearance associated with severe anemia (Fig. 5Ci and Cii). Here, parasite elimination results in the alteration of uninfected erythrocytes to limit their filtration through the spleen as well as to potentiate their removal by activated macrophages.

Elevation of the CD8$^+$ T cell response associated with SMA in a case-control pediatric cohort infected with *P. falciparum*. Since the rat model is expected to better mimic the pathophysiology of human disease, the relevance of our findings to patient populations was investigated in a case-control pediatric cohort from Ibadan, Nigeria. The study design and details of clinical case definition are included in Materials and Methods. As shown in

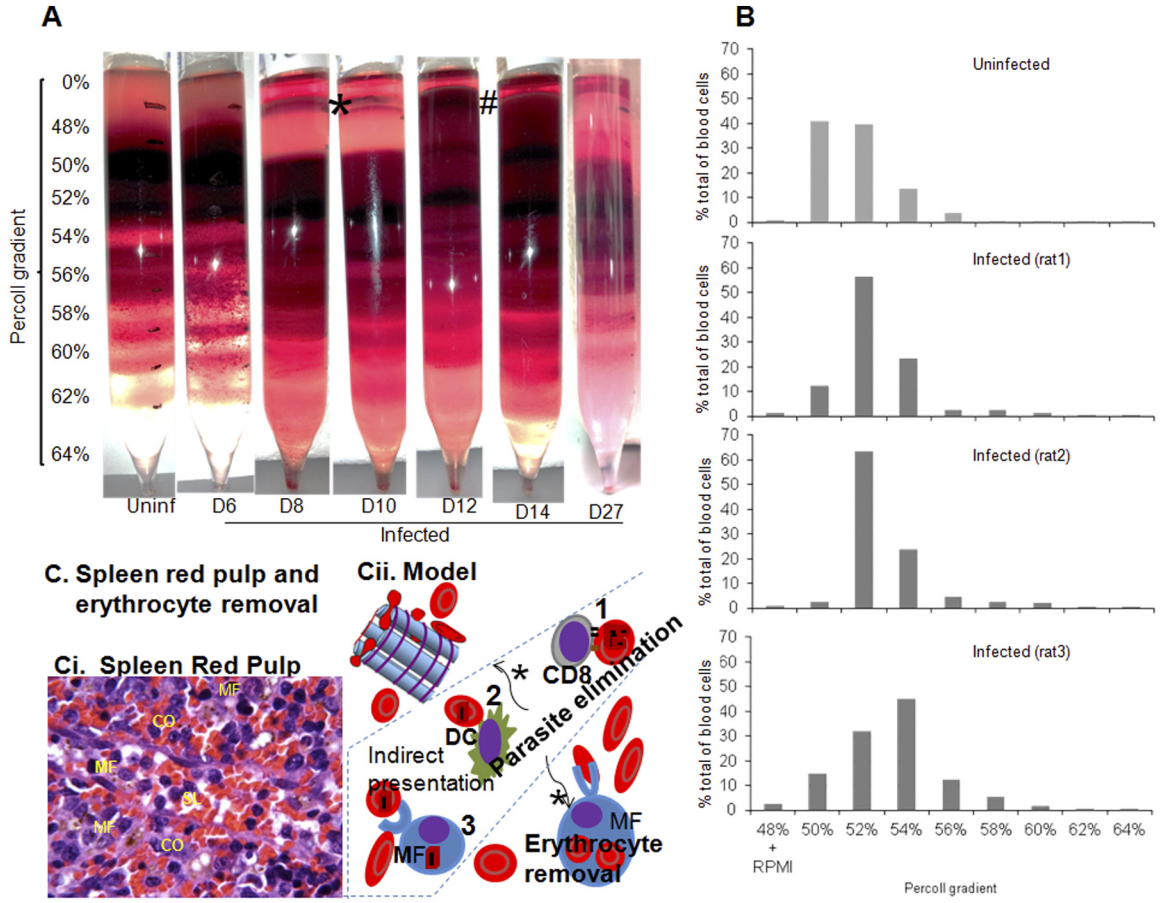

FIG 5 Properties of uninfected erythrocytes are altered in the *P. berghei* ANKA infection/anemia model. (A) Visual representation of total blood obtained from uninfected (Uninf) and infected rats fractionated on Percoll density gradients on the indicated days after the onset of infection. On these gradients, infected erythrocytes (∗ in panel A) and reticulocytes (# in panel A) are detected in the top light fraction (48% Percoll), while uninfected erythrocytes are detected at intermediate and higher densities (50% and greater). (B) Cell counts of the different density fractions suggest that infection increases with the relative density of uninfected erythrocytes. Analyses shown for blood from an uninfected rat and three individual infected rats at day 12 (a time of active erythrocyte removal and production of new reticulocytes marked by #) indicates that uninfected erythrocytes from all three infected animals were consistently detected in the higher-density fractions of 54%, 58%, and 60% Percoll. (C) Spleen red pulp and a model for erythrocyte removal. (Ci) H&E stain of infected spleen red pulp showing high concentrations of erythrocytes (red), macrophages (MF), cords (CO), and sinus lumen (SL). (Cii) Multiple mechanisms of erythrocyte removal in the spleen. Parasite killing in the red pulp, through direct mechanisms ($CD8^+$ T cell dependent [no. 1]) and indirect mechanisms (such as presentation via dendritic cells and macrophages [no. 2 and 3]) may activate macrophages to trigger erythrocyte removal. Parasite killing may also induce changes in uninfected-erythrocyte properties, further enhancing their removal by activated macrophages (∗). Changes in erythrocyte properties may limit their squeezing (∗) through the sinusoids (blue barrel), resulting in entrapment in the red pulp and subsequent removal there. All three processes are likely to work in conjunction, leading to SMA.

Fig. 6, plasma specimens from 268 children between the ages of 6 and 149 months (13 years) were analyzed. Two hundred eleven *P. falciparum*-infected children without neurological symptoms were separated on the basis of packed cell volume (PCV) into the SMA group (PCV, 5 to 15%; $n = 48$) and uncomplicated malaria (UM) group (PCV, 16 to 45%; $n = 163$). The UM group was further subdivided into groups with acute infection with no malarial anemia (AINMA) (PCV, 29 to 45%; $n = 92$) and mild malarial anemia (MMA) (PCV, 16 to 28%; $n = 71$). Also included were plasma samples from 57 age-matched community controls (CC) (PCV, 30 to 42%).

P. falciparum histidine-rich protein 2 (PfHRP2), the lead marker used to estimate total parasite mass (6, 7), was detected in over 89% of patient samples across disease groups (Fig. 6A). We found that higher plasma concentrations of PfHRP2 (and not peripheral parasitemia) were associated with SMA (Fig. 6B, section I). When the UM (AINMA and MMA) and SMA groups were combined, PCV levels inversely and significantly correlated with plasma levels of PfHRP2 ($r =$ to 0.43; $P < 0.0001$) or with estimated total parasite biomass ($r =$ to 0.42; $P < 0.0001$).

sCD8 was also significantly increased for SMA patients compared to levels in the CC ($P = 0.004$), AINMA ($P = 0.09$), or MMA ($P = 0.021$) group, although there was considerable variation in the data in all groups (Fig. 6B, section II). In humans, $CD8^+$ T cell levels may reflect responses to liver infection (although this will not be reflected in the PfHRP2 biomass). Nonetheless, a univariate logistic regression analysis indicated that age (odds ratio [OR], 0.3-fold; 95% confidence intervals [$CI_{95\%}$], 0.2- to 0.6-fold) and weight (OR, 0.4-fold; $CI_{95\%}$, 0.2- to 0.7-fold]) were significantly associated with a decreased risk of SMA in children (Table 1). However, this risk increased when the plasma concentrations of PfHRP2 (OR, 3.5-fold; $CI_{95\%}$, 1.7- to 7.1-fold) (but not peripheral parasitemia) or the estimated total parasite biomass (OR, 3.7-fold; $CI_{95\%}$, 1.8- to 7.5-fold) (but not the number of

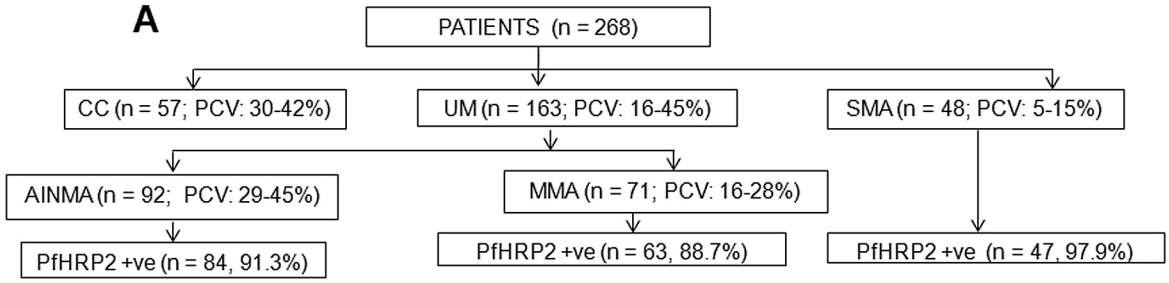

B

Characteristics	CC (n = 42)	UM AINMA (n = 84)	UM MMA (n = 63)	SMA (n = 47)
Sex (M/F)	18/24	47/36	39/24	29/18
Age (year), Mean (range)	**5.4** (0.7 - 13)	**5.6** (0.5 - 12)	**3.9** (0.7 - 11)	**3.2** (0.7 - 12.4)
Weight (kg), Mean (range)	**17.8** (6 - 40)	**18.6** (6 - 36)	**14.5** (8 - 27)	**13.2** (6 - 30)
PCV, Mean (range)	**34.9** (30 - 42)	**34.4** (29 - 45)	**23.5** (16 - 28)	**12.3** (5 - 15)
Parasite/μL Mean (95% CI) (range)	0	**9857** (33024 - 54578) (0 - 219608)	**20634** (47789 - 76730) (94 - 220583)	**14858** (41495 - 74962) (0 - 186139)
I. PfHRP2, ng/mL Median (range)	-	**69** (0-1767)	**247** (4-4751)	**473** (49-17155)
Tot. Par. Bdn($x10^{11}$) Median (range)	-	**0.6** (0.0022 - 23)	**1.7** (0.029 - 38)	**4.8** (0.31 - 109.3)
Cir. Par. Bdn($x10^{11}$) Median (range)	-	**0.3** (0.000015 -5.6)	**0.6** (0.0011 - 3.2)	**0.4** (0.0000072 – 2.0)
Sequestration Index Median (range)		**2.7** (0.01-430)	**4.0** (0.05-4888)	**14.1** (0.46-8302)
II. sCD8, pg/mL Median (range)	**314** (23-1037)	**307** (12-6042)	**330** (27-4155)	**472** (60-7502)

FIG 6 Total parasite burden and sCD8 as correlates of SMA in a case-control pediatric cohort infected with *P. falciparum*. (A) Diagrammatic representation of patient groups, with numbers of children and PCV cutoffs used to assign them to the SMA group and the uncomplicated malaria (UM) group (which was further subdivided into patients with acute infection and no malarial anemia [AINMA] and mild malarial anemia [MMA]). (B) For each patient group, clinical parameters and plasma levels of PfHRP2, from which the total parasite burden (Tot. Par. Bdn) and sequestration index (from the expected PfHRP2 level) were calculated as previously described (6, 7, 45) (section I), and sCD8 (section II). Cir. Par. Bdn, circulating parasite burden.

circulating parasites) were elevated. The risk of SMA also increased when plasma sCD8 (OR, 2.4-fold; $CI_{95\%}$, 1.0- to 5.7-fold) was elevated (Table 1). Notably, the concomitant elevation in both plasma parameters was associated with a significant increased risk of SMA (OR, 7.2-fold; $CI_{95\%}$, 1.9- to 27.4-fold), suggesting that activated $CD8^+$ T cells and parasite biomass may act in conjunction, as predicted from the rat model. In infected children, this association was observed even after adjustment for age and weight (adjusted OR, 6.7-fold; $CI_{95\%}$, 1.7- to 25.7-fold) (Table 1).

DISCUSSION

Multiple host factors are known to influence malarial anemia (2, 23), but these are innate mechanisms (4, 24, 25). *P. berghei*-infected rats have historically been used to study anemia (26, 27). The rat spleen confers T cell immunity (28). $CD4^+$ T cells were proposed to eliminate anemia in a murine malaria model (8), but the study lacked quantitation of both $CD4^+$ and $CD8^+$ T cells. The same study also suggested that uninfected erythrocytes taken from anemic rats show normal clearance in uninfected rats, but we find that anemia is intrinsic to the infected spleen. Prior evidence indicates that $CD8^+$ and/or $CD4^+$ T cells may influence parasite biomass/infection in *P. berghei* and other malarias in rodents (29–33). Our data from the rat model show that the $CD8^+$ T cells regulate parasite clearance and anemia as an adaptive (rather than an innate) immune response in the spleen. In future studies, splenectomized rats may be used to further confirm the key role of the spleen, with the caveat that circulating parasitemias may be substantially higher.

With respect to mechanisms of anemia, our depletion experiments suggest that $CD4^+$-activated NK cells are not likely to be involved in parasite killing. Rather $CD8^+$ T cell-induced parasite clearance may generate an intermediate(s) that stimulates innate clearance mechanisms of macrophages to trigger erythrocyte removal in the spleen (Fig. 5C). Moreover, infection changes properties of a large number of uninfected erythrocytes. This may further facilitate their uptake by activated macrophages as well as limit filtration through the splenic sinusoids, resulting in entrapment in the RP, and thus additionally potentiate clearance there (Fig. 5C). This may be due to steric or antigenic changes in uninfected erythrocytes that may be investigated in *in vitro* studies. Thus, although their exact nature has yet to be determined, changes in uninfected-erythrocyte properties may signify mechanisms of removal in the spleen analogous to those seen with inherited anemias (34).

TABLE 1 sCD8 is a risk factor for SMA and shows synergy with PfHRP2 for development of a dual, preferred, predictive index of SMA[a]

Characteristic	OR	$CI_{95\%}$ (fold)	*P* value
Sex			
Male	1		
Female	0.9	0.5–1.8	0.79
Age (yr)			
Lower	1		
Higher	0.3	0.2–0.6	0.001
Weight (kg)			
Lower	1		
Higher	0.4	0.2–0.7	0.003
Parasitemia (%)			
Lower	1		
Higher	1.4	0.7–2.8	0.29
Plasma PfHRP2 (ng/ml)			
Lower	1		
Higher	3.5	1.7–7.1	0.0005
Plasma sCD8 (μg/ml)			
Lower	1		
Higher	2.4	1.0–5.7	0.04
Circulating parasite biomass			
Lower	1		
Higher	0.8	0.4–1.6	0.58
Total parasite biomass			
Lower	1		
Higher	3.7	1.8–7.5	0.0004
Plasma samples with CD8-PfHPR2			
Lower-lower	1		
Higher-lower	2.2	0.5–9.3	0.30
Lower-higher	2.8	0.6–12.1	0.17
Higher-higher	7.2	1/9/27.4	0.004
Multivariate logistic regression			
Plasma samples with CD8-PfHPR2			
Lower-lower	1		
Higher-lower	2.1[b]	0.5–8.9	0.33
Lower-higher	2.6[b]	0.6–11.4	0.20
Higher-higher	6.7[b]	1/7/25.7	0.006

[a] Univariate logistical-regression analysis was undertaken to determine the odds ratio (OR) associated with the risk of SMA for age, weight, PfHRP2 level, estimated total parasite biomass, circulating parasites in the blood, and plasma sCD8.
[b] Adjusted values were used for age and weight.

Upon parasite clearance in humans, $CD8^+$ T cell responses are clearly directly elicited by liver-stage infection (20, 21, 35, 36). Activation by blood-stage infection has also been suggested (36, 37). In our studies, the infections bypass the liver stage. Prior studies suggest that murine $CD8^+$ T cells recognize blood-stage rodent malaria parasites (22, 38). Dendritic cells may contribute and be present in preparations of $CD8^+$ T cells (but in our studies, immunodepletion of animals with anti-CD8α did not deplete $CD8^+$ dendritic cells). There may be additional mechanisms of activation, such as exosomes derived from infected reticulocytes (39). We find that the increase in $CD8^+$ T cells is directly proportional to parasite biomass in the spleen. We find sCD8 to be a strong surrogate for $CD8^+$ T cells. Since the plasma volumes required are small, dual assessment of sCD8 and PfHRP2 parasite burden may be readily expanded to larger clinical studies for identification of patients at greatest risk for SMA.

In malaria, anemia requires persistent parasite clearance, likely ongoing in semi-immune parasitemic individuals. Our work shows that in pediatric patients, the $CD8^+$ host response can independently increase the risk of SMA. Moreover, the host response and parasite burden can be synergized in severe-disease predictions. It will be important to engineer a highly protective $CD8^+$ T cell response in the presence of minimal parasite loads to reduce the risk of anemia, which has been frequently associated with the challenge phase of testing malaria vaccines (40–42).

MATERIALS AND METHODS

Wistar rat model of *P. berghei* infection and anemia. BALB/c mice were first injected intraperitoneally (i.p.) with thawed stabilates of blood-stage *P. berghei* ANKA. Subsequently, live parasites isolated from mice were used to infect aged Wistar rats. Fifteen-week-old rats were injected i.p. with 10^6 wild-type or Δ*msp7* mutant parasites (10). Parasitemia, hemoglobin, and other blood parameters were monitored every 2 days. Parasite levels were monitored by performing Giemsa staining of thin blood film or qPCR, and hemoglobin (Hb) levels were determined by the method of Drabkins (as noted in reference 10).

Microarray experiments and data analysis. Spleens from 2 wild-type-parasite-infected, 2 Δ*msp7* mutant-infected, and 2 uninfected rats (15 weeks of age) were surgically harvested, kept in RNAlater, and stored at −20°C until used. RNA was isolated using a Roche MagNA Pure compact automated system, and labeling was done using a MessageAmp Premier RNA amplification kit (Invitrogen). Affymetrix rat 430 2.0 array hybridizations were performed by the UCLA Clinical Microarray Core, UCLA, Los Angeles, CA, according to the standard Affymetrix GeneChip expression analysis protocol. RNA from each animal was profiled individually. Thresholds for selecting significant genes were set at a relative difference of ≥1.5-fold, an absolute difference of ≥100 signal intensity units, and a *P* of <0.05. Genes that met all three criteria were considered significantly changed.

General histopathology and analysis. Spleen, liver, lung, brain, and kidney were harvested from rats not infected or infected with wild-type or Δ*msp7* parasites. Harvested organs were cut into smaller portions and placed into fixative (10% neutral buffered formalin) for at least 48 h at room temperature. Samples were then processed and paraffin embedded at AML Laboratories Inc. (Baltimore, MD), and thin sections (3 to 4 μm) were produced with a microtome and stained with hematoxylin and eosin (H&E).

Immunohistochemistry and imaging. Mouse monoclonal antibodies (MAbs) utilized were anti-rat (i) CD8α (clone OX-8, catalog no. MCA48G), (ii) CD4 (clone W3/25, no. MCA55R), (iii) CD68 (clone ED1, no. MCA341R; AbD Serotec, Oxford, United Kingdom), and (iv) OX 62 for dendritic cells (DC) (clone OX-62, no. MCA1029GA; AbD Serotec, Oxford, United Kingdom; also referred to as anti-DC). Formalin paraffin-embedded spleen or liver sections (3 to 4 μm) were dewaxed in xylene. For samples probed by MAbs anti-CD4, anti-CD68, and anti-DC, antigen retrieval required preincubation of deparaffinized samples with 0.05% proteinase K (Dako, Hamburg, Germany; no. S3004) in 0.05 mol/liter Tris-HCl (pH, 7.5) for 8 min at room temperature (RT). After being washed, sections were immersed in 3% H_2O_2 in phosphate-buffered saline (PBS) for 20 min at RT to block endogenous peroxidase. After an additional wash, the sections were treated with 5% horse serum for 30 min, followed by successive incubation in avidin and biotin (no. SP-2001 avidin/biotin blocking kit; Vector Laboratories) to block endogenous biotin. Anti-CD8α (dilution, 1/100), anti-CD4 (dilution, 1/100), anti-CD68 (dilution, 1/500), or anti-DC (dilution, 1/100) was applied to the sections in PBS with 1% horse serum and kept overnight at 4°C (for MAbs anti-CD8, anti-CD4, and anti-DC) or for 60 min at RT (for MAb anti-CD68). Affinity-purified, biotinylated, and rat absorbed horse anti-mouse IgG (no. BA-2001) and the Vectastain ABC Elite system for peroxidase (no. PK 6102) were from Vector Laboratories (Burlingame, VT, USA). The Ab was used to detect anti-CD8α, anti-CD4, anti-CD68, or anti-DC in all samples. Reagents were prepared according to the manufacturers' recommendations. The peroxidase complexes were revealed by incubation with 3,3′-diaminobenzidine-tetra-hydrochloride (DAB; substrate no. SK-4100; Vector Laboratories) or Vector NoraRED (no. SK-4800; Vector Laboratories), and the sections were lightly counterstained

with Mayer's hemalum. The slides were then mounted in Cytoseal XYL (no. 8312-4; Thermo Scientific, Kalamazoo, MI, USA). Incubations for negative controls were carried out with sections incubated with normal mouse IgG1 (no. MCA1209; AbD Serotec, Oxford, United Kingdom) or in the absence of the primary antibody.

For each spleen slide, images were collected within the follicle (white pulp [WP]) and the adjacent marginal zone (MZ; marginal sinus included) and red pulp (RP). Follicles with a clear differentiation between the white pulp, the adjacent MZ, and the RP were selected for imaging. The collection of the images was done at a magnification of ×1,000 (high-power fields [HPF]). The images of all areas of the follicle and the adjacent MZ were collected, while at least 10 randomly selected fields in the adjacent RP around the follicle were collected. Pictures were acquired on a Nikon Olympus microscope using a Nikon digital DS-Fi1-U2 camera controlled by NIS-Elements F3.0 Nikon software (all from Nikon Instruments Inc., Tokyo, Japan). Images were visualized with a DPIan Apo 40×/1.00 oil immersion or a DPIan Apo 100×/1.30 oil immersion objective lens (Nikon). For each sample, positive cells were counted and localized on at least two follicles with the adjacent MZ and RP.

For each liver slide, images were collected within the entire tissue sample at a magnification of ×1,000. For each type of cellular stain ($CD8^+$ T cells, $CD4^+$ T cells, $CD68^+$ cells, or DC), more than 600 photographs were analyzed. The densities of $CD8^+$ T cells, $CD4^+$ T cells, $CD68^+$ cells, or DC were estimated as the number of positive cells per HPF.

Live-cell immunofluorescence assay. Fluorescein isothiocyanate (FITC) mouse monoclonal anti-rat RT1A (clone OX-18, catalog no. 554919; BD Biosciences, USA) was used to detect MHC class I. Phycoerythrin (PE) mouse anti-rat CD71 (clone OX-26, no. 554891) was used to detect rat CD71. Fresh blood was collected, washed with PBS (pH = 7.4), and then incubated with anti-RT1A and anti-CD71 (4 μg/ml) diluted in PBS-bovine serum albumin (BSA; 2%) for 30 min on ice under slight agitation. After five washes with PBS, cell nuclei were stained with 4′,6-diamidino-2-phenylindole (DAPI) for 5 min. Cells were then washed with PBS and fixed with PBS-formaldehyde (1%). Slides were mounted with Vectashield medium (Vector Laboratories, Burlingame, CA) for imaging. Images were visualized with a 100× oil immersion objective lens and captured using an inverted Olympus IX fluorescence microscope and a CoolSnap HQ2 charge-coupled-device (CH350/LCCD) camera controlled by DeltaVision software (Applied Precision, Seattle, WA).

Percoll density gradients. Discontinuous Percoll density gradients (Sigma-Aldrich, St. Louis, MO, USA) consisting of 1.5-ml fractions, with densities ranging from 48 to 64% Percoll in RPMI medium, were assembled as indicated in Fig. 5A. Peripheral blood was collected from uninfected and infected animals, washed three times, and diluted in RPMI medium (hematocrit = 80%). From this suspension, 1 ml was layered on the Percoll gradient and separated by centrifugation at 3,000 rpm for 40 min at 19°C. Fractions were collected by careful pipetting. The number of cells per fraction was counted using a Malassez chamber.

RNA extraction. For each spleen sample, three sections (5 μm each) separated by 50 μm were collected and pooled for RNA extraction. Total RNA was extracted with an RNeasy FFPE kit (reference no. 73504; Qiagen) according to the manufacturer's instructions. RNA extracts were quantified using a NanoDrop ND-1000 (NanoDrop Technologies, Wilmington, DE, USA). The integrity of the RNA was controlled with an RNA nano chip (2100 Bioanalyzer; Agilent Biotechnologies, Wilmington, DE). Samples were immediately stored at −20°C.

Quantitative real-time PCR. Primers were designed from the *P. berghei* Anka 18S rRNA gene (GenBank accession no. AJ243513.1) and the rat GAPDH (glyceraldehyde-3-phosphate dehydrogenase) gene (GenBank accession no. NM_017008). The sequence of the specific primers for *P. berghei* 18S RNA and rat GAPDH were 18S RNA forward (5′ AATCT TGAACGAGGAATGCCTAGT 3′), 18S RNA reverse (5′ ACGGGCGGT GTGTACAAAG 3′), GAPDH forward (5′ TGGCCTCCAAGGAGTAAG AAAC 3′), and GAPDH reverse (5′ GGCCTCTCTCTTGCTCTCAGTAT C 3′). Amplification of the GAPDH sequence served as the internal control for normalization. qPCR was performed using the 7900 HT Fast real-time PCR system (Applied Biosystems) with a 20-μl reaction volume and the Power SYBR Green RNA-to-CT one-step kit (catalog reference no. 4389986; Applied Biosystems). Serial dilutions of the cDNA (1:1, 1:10, 1:100, 1:1,000, 1:10,000) with nuclease-free water (reference no. AM9935; Applied Biosystems) were used to generate a relative standard curve for 18S RNA as well as GAPDH. The concentrations of target sequence in the samples are extrapolated from the standard curve. The quantities were normalized by dividing the quantity of the 18S RNA by the quantity of the GADPH.

Spleen lymphocyte isolation and characterization by flow cytometry. To isolate lymphocytes, spleens were harvested from rats infected with wild-type and Δ*msp7* mutant parasites on day 8 and day 10. Total splenocytes were isolated, erythrocytes were lysed, and residual cells were stained for B (CD45RA), NK (CD161a), and CD3 (CD4 and CD8) cells. Subsets of cells were identified by first gating them on lymphocytes by forward and side scatter. CD3 singly positive cells were then analyzed for CD4 and CD8 expression. A suitable isotype control for each antibody was included as a control, and compensation was performed wherever required. Events were recorded in a Beckman Coulter FC500 flow cytometer and data analyzed with FlowJo.

***In vitro* stimulation of $CD8^+$ T cells with wild-type parasites.** Whole blood was separated in two parts, one for peripheral blood mononucleated cells (PBMCs) and $CD8^+$ T cell purification and the other part for infected-erythrocyte purification. Erythrocytes were lysed with NH_4Cl, and the cells were washed twice in fresh medium. $CD8^+$ T cells were purified with positive selection using a magnetically activated cell sorting (MACS) cell separation system (Miltenyi Biotech, USA) according to the manufacturer's protocols. The purity of $CD8^+$ T was 95%. Infected erythrocytes were obtained as described previously (43).

For the *in vitro* stimulation assay, 10^6 purified $CD8^+$ T cells were stimulated with 10^5 purified infected erythrocytes (with ~40% infected reticulocytes) suspended in 200 μl incubation medium (RPMI 1640 plus L-glutamine plus neomycin plus 30% fetal bovine serum) for 72 to 82 h, and the levels of IFN-γ in the supernatant were determined by a sandwich enzyme-linked immunosorbent assay (ELISA). Uninfected erythrocytes and staphylococcal enterotoxin B antigen (SEB; 5 μg/ml; Sigma) were used as negative and positive controls, respectively.

Animal procedures. Animal protocols were reviewed and approved by the institutional animal care and use committees of Northwestern University (protocol no. 2006-0935) and the University of Notre Dame (protocol no. 11-070).

Ethics statement. Parents or guardians of study participants gave informed written consent. The research was approved by the internationally accredited joint ethics committees of the College of Medicine of the University of Ibadan and the University College Hospital, Ibadan, Nigeria. All procedures with human subjects were approved by the Institutional Review Board of the University of Notre Dame.

Patient study design and sample collection. All study participants of this case-control study were recruited during 2009 to 2012. Children with malaria were recruited by the Childhood Malaria Research Group (CMRG) at the University College Hospital (UCH), Ibadan, Nigeria. Community control (CC) children (malaria negative) were recruited from local vaccination clinics and school visits from multiple districts of Ibadan.

The children were from 6 months to 13 years old. They were screened for parasite detection by microscopy following Giemsa staining of thick and thin blood films as performed routinely at the UCH. Clinical definitions used were as indicated by the WHO criteria for severe *P. falciparum* malaria (44). All infected children were positive for *P. falciparum*. Uncomplicated malaria (UM) cases were additionally defined as febrile with a PCV (packed cell volume) of >20% (not requiring hospital admission). Severe malarial anemia (SMA) cases showed PCVs of <16%. CC children appeared healthy, without any disease symptoms. They were *P. falciparum* negative in both thick and thin Giemsa smears and selected for age and sex

match with the patient group. The clinical data were compiled for each patient; blood samples were collected in an EDTA tube, and the plasma was separated (1,000 × *g*, 10 min), aliquoted, and frozen at −80°C until used.

Quantitative analyses of PfHRP2, parasite biomass, the sequestration index, and sCD8. The quantification of *P. falciparum* histidine-rich protein 2 (PfHRP2) in the plasma of malaria patients was carried out by sandwich ELISA essentially as previously described (6). Briefly, the mouse monoclonal Ab anti-*P. falciparum* HRP2 IgM (MPFM-55A; Immunology Consultants Laboratory Inc., USA) and horseradish peroxidase (HRP)-conjugated anti-*P. falciparum* IgG (MPFG-55P; Immunology Consultants Laboratory Inc., USA) were used for plate coating and for detection, respectively. The detection limit of the assay was 31.25 pg/ml. Positive cases were defined as those in which duplicate derived concentrations were greater than the detection limit. Each ELISA plate contained samples from UM patients and from age-matched SMA patients.

Circulating and whole-body parasite biomasses were calculated using the previously reported formulas (6, 7). Total parasite biomass was calculated only from individuals with detectable PfHRP2 in the plasma. The sequestration index was calculated as the total parasite burden divided by the circulating burden (45).

Plasma sCD8 ELISA. Plasma quantification of sCD8 was done by a sandwich ELISA using the mouse monoclonal antibody anti-human CD8α (clone D-9, sc-7970; Santa Cruz Biotechnology, Inc.), which recognizes both human and rat sCD8, as the primary antibody and the rabbit polyclonal antibody anti-human CD8α (clone H-160, sc-7188; Santa Cruz Biotechnology, Inc.) as the secondary antibody; these were detected by the HRP-conjugated goat polyclonal Ab anti-rabbit IgG (H+L) (PI-1000; Vector Laboratories). Each ELISA plate contained samples from CC patients and from age-matched UM and SMA patients.

Statistical analysis. The Wilcoxon signed-rank test for matched pairs was used to compare continuous outcomes at different time points. The Mann-Whitney U test, Student's *t* test, Kruskal-Wallis test, or one-way analysis of variance (ANOVA) with a Tukey or Bonferroni *post hoc* analysis was used to compare continuous outcomes of different groups at the same time point. The correlation between different continuous measures was determined using the Spearman correlation coefficient.

SMA risk factors were evaluated using univariate and multivariate logistic-regression models. The binary outcome (yes/no) was a dependent variable. Eight independent variables were studied: sex, age, body weight, peripheral parasitemia, plasma concentrations of PfHRP2 and sCD8, and the estimated circulating and total parasite biomasses. Apart from sex, all independent variables were coded as binary (high or low according to the median). Since in the rat model we show that concomitant increases of parasite clearance and $CD8^+$ T cell number predict anemia, we defined another independent variable, which is the combination of plasma concentrations of PfHRP2 and sCD8. This last variable has 4 classes according to the median (low and high for plasma concentrations of both sCD8 and PfHRP2, low plasma concentrations of sCD8 and high concentrations of PfHRP2, and high plasma concentrations of sCD8 and low concentrations of PfHRP2). The effects of independent variables for the risk of developing SMA were evaluated using unconditional univariate regression analysis. The factors significant at a level of 0.05 in the univariate analysis were then included in a multivariate logistic model. All statistical analyses were performed with SPSS statistical software (PASW statistic version 18). All *P* values were two sided, and those <0.05 were considered significant.

SUPPLEMENTAL MATERIAL

Supplemental material for this article may be found at http://mbio.asm.org/lookup/suppl/doi:10.1128/mBio.02493-14/-/DCSupplemental.

Figure S1, PDF file, 0.3 MB.
Figure S2, GIF file, 0.5 MB.
Figure S3, GIF file, 0.9 MB.
Figure S4, PDF file, 0.5 MB.
Figure S5, PDF file, 0.2 MB.
Figure S6, PDF file, 0.02 MB.
Table S1, PDF file, 0.01 MB.
Table S2A, XLS file, 0.1 MB.
Table S2B, XLS file, 0.03 MB.
Table S3, PDF file, 0.03 MB.

ACKNOWLEDGMENTS

We thank Souvik Bhattacharjee for recombinant HRP2 and Trupti Pandharkar for comparative analysis of rat and murine genes and bioinformatic analyses.

This work was supported by the NIH (grants P01 HL078826 to K.H., A.H., N.M., P.B., and R.T.; R0HL069630 and R01AI039071 to K.H.; and F31 HL09277 to N.D.G.) and the UK Medical Research Council (grants U117532067 to A.H. and D.F.-R. and G0900109 to R.T.). The authors declare no competing financial interests.

Innocent Safeukui, Rama Akondy, David Olaleye, Rafi Ahmed, Anthony Holder, Olugbemiro Sodeinde, James Kazura, Narla Mohandas, Delmiro Fernandez-Reyes, and Kasturi Haldar designed the research; Innocent Safeukui, Noé D. Gomez, Aanuoluwa A. Adelani, Florence Burte, Nathaniel K. Afolabi, Rita Tewari, and Biobele J. Brown performed the research; Innocent Safeukui, Noé D. Gomez, Aanuoluwa A. Adelani, Florence Burte, Nathaniel K. Afolabi, Rita Tewari, Rafi Ahmed, Anthony Holder, Rita Tewari, Pierre Buffet, Biobele J. Brown, Wuraola A. Shokunbi, David Olaleye, Olugbemiro Sodeinde, James Kazura, Rafi Ahmed, Narla Mohandas, Delmiro Fernandez-Reyes, and Kasturi Haldar analyzed the data and interpreted the results; Nathaniel K. Afolabi, Biobele J. Brown, Wuraola A. Shokunbi, David Olaleye, Olugbemiro Sodeinde, and Delmiro Fernandez-Reyes recruited malaria patients and analyzed clinical data; Innocent Safeukui performed statistical analyses; Innocent Safeukui, Rama Akondy, Anthony Holder, Rita Tewari, Pierre Buffet, Biobele J. Brown, Wuraola A. Shokunbi, David Olaleye, Olugbemiro Sodeinde, James Kazura, Rafi Ahmed, Narla Mohandas, Delmiro Fernandez-Reyes, and Kasturi Haldar wrote the paper; and Peter Velazquez, designed the research, analyzed the data, and interpreted the results.

REFERENCES

1. **WHO.** 2012. Malaria report 2012. **WHO, Geneva,** Switzerland. http://www.who.int/malaria/publications/world_malaria_report_2012/wmr2012_summary_en.pdf.
2. **Miller LH, Baruch DI, Marsh K, Doumbo OK.** 2002. The pathogenic basis of malaria. Nature **415:**673–679. http://dx.doi.org/10.1038/415673a.
3. **Menendez C, Fleming AF, Alonso PL.** 2000. Malaria-related anaemia. Parasitol Today **16:**469–476. http://dx.doi.org/10.1016/S0169-4758(00)01774-9.
4. **Buffet PA, Safeukui I, Deplaine G, Brousse V, Prendki V, Thellier M, Turner GD, Mercereau-Puijalon O.** 2011. The pathogenesis of Plasmodium falciparum malaria in humans: insights from splenic physiology. Blood **117:**381–392. http://dx.doi.org/10.1182/blood-2010-04-202911.
5. **Hedberg K, Shaffer N, Davachi F, Hightower A, Lyamba B, Paluku KM, Nguyen-Dinh P, Breman JG.** 1993. Plasmodium falciparum-associated anemia in children at a large urban hospital in Zaire. Am J Trop Med Hyg **48:**365–371. http://www.ajtmh.org/content/48/3/365.long..
6. **Dondorp AM, Desakorn V, Pongtavornpinyo W, Sahassananda D, Silamut K, Chotivanich K, Newton PN, Pitisuttithum P, Smithyman AM, White NJ, Day NP.** 2005. Estimation of the total parasite biomass in acute falciparum malaria from plasma PfHRP2. PLoS Med **2:**e204. http://dx.doi.org/10.1371/journal.pmed.0020204.
7. **Hendriksen IC, Mwanga-Amumpaire J, von Seidlein L, Mtove G, White LJ, Olaosebikan R, Lee SJ, Tshefu AK, Woodrow C, Amos B, Karema C, Saiwaew S, Maitland K, Gomes E, Pan-Ngum W, Gesase S, Silamut K, Reyburn H, Joseph S, Chotivanich K, Fanello CI, Day NP, White NJ, Dondorp AM.** 2012. Diagnosing severe falciparum malaria in parasitaemic African children: a prospective evaluation of plasma PfHRP2 measurement. PLoS Med **9:**e1001297. http://dx.doi.org/10.1371/journal.pmed.1001297.
8. **Evans KJ, Hansen DS, van Rooijen N, Buckingham LA, Schofield L.** 2006. Severe malarial anemia of low parasite burden in rodent models results from accelerated clearance of uninfected erythrocytes. Blood **107:**1192–1199. http://dx.doi.org/10.1182/blood-2005-08-3460.

9. **Lamikanra AA, Brown D, Potocnik A, Casals-Pascual C, Langhorne J, Roberts DJ.** 2007. Malarial anemia: of mice and men. Blood **110:**18–28. http://dx.doi.org/10.1182/blood-2006-09-018069.
10. **Gómez ND, Safeukui I, Adelani AA, Tewari R, Reddy JK, Rao S, Holder A, Buffet P, Mohandas N, Haldar K.** 2011. Deletion of a malaria invasion gene reduces death and anemia, in model hosts. PLoS One **6:**e25477. http://dx.doi.org/10.1371/journal.pone.0025477.
11. **Thawani N, Tam M, Bellemare MJ, Bohle DS, Olivier M, de Souza JB, Stevenson MM.** 2014. Plasmodium products contribute to severe malarial anemia by inhibiting erythropoietin-induced proliferation of erythroid precursors. J Infect Dis **209:**140–149. http://dx.doi.org/10.1093/infdis/jit417.
12. **Millot S, Andrieu V, Letteron P, Lyoumi S, Hurtado-Nedelec M, Karim Z, Thibaudeau O, Bennada S, Charrier JL, Lasocki S, Beaumont C.** 2010. Erythropoietin stimulates spleen BMP4-dependent stress erythropoiesis and partially corrects anemia in a mouse model of generalized inflammation. Blood **116:**6072–6081. http://dx.doi.org/10.1182/blood-2010-04-281840.
13. **Chen LT.** 1980. Intrasplenic microcirculation in rats with acute hemolytic anemia. Blood **56:**737–740. http://www.bloodjournal.org/content/56/4/737.long..
14. **Deplaine G, Safeukui I, Jeddi F, Lacoste F, Brousse V, Perrot S, Biligui S, Guillotte M, Guitton C, Dokmak S, Aussilhou B, Sauvanet A, Cazals Hatem D, Paye F, Thellier M, Mazier D, Milon G, Mohandas N, Mercereau-Puijalon O, David PH, Buffet PA.** 2011. The sensing of poorly deformable red blood cells by the human spleen can be mimicked in vitro. Blood **117:**e88–e95. http://dx.doi.org/10.1182/blood-2010-10-312801.
15. **Safeukui I, Correas JM, Brousse V, Hirt D, Deplaine G, Mulé S, Lesurtel M, Goasguen N, Sauvanet A, Couvelard A, Kerneis S, Khun H, Vigan-Womas I, Ottone C, Molina TJ, Tréluyer JM, Mercereau-Puijalon O, Milon G, David PH, Buffet PA.** 2008. Retention of Plasmodium falciparum ring-infected erythrocytes in the slow, open microcirculation of the human spleen. Blood **112:**2520–2528. http://dx.doi.org/10.1182/blood-2008-03-146779.
16. **Best JA, Blair DA, Knell J, Yang E, Mayya V, Doedens A, Dustin ML, Goldrath AW, The Immunological Genome Project Consortium.** 2013. Transcriptional insights into the CD8$^+$ T cell response to infection and memory T cell formation. Nat Immunol **14:**404–412. http://dx.doi.org/10.1038/ni.2536.
17. **Fujimoto J, Levy S, Levy R.** 1983. Spontaneous release of the leu-2 (T8) molecule from human T cells. J Exp Med **158:**752–766. http://jem.rupress.org/content/158/3/752.long. http://dx.doi.org/10.1084/jem.158.3.752.
18. **Tomkinson BE, Brown MC, Ip SH, Carrabis S, Sullivan JL.** 1989. Soluble CD8 during T cell activation. J Immunol **142:**2230–2236. http://www.jimmunol.org/content/142/7/2230.long..
19. **Kenny E, Mason D, Saoudi A, Pombo A, Ramírez F.** 2004. CD8 alpha is an activation marker for a subset of peripheral CD4 T cells. Eur J Immunol **34:**1262–1271. http://dx.doi.org/10.1002/eji.200324363.
20. **Overstreet MG, Cockburn IA, Chen YC, Zavala F.** 2008. Protective CD8 T cells against plasmodium liver stages: immunobiology of an "unnatural" immune response. Immunol Rev **225:**272–283. http://dx.doi.org/10.1111/j.1600-065X.2008.00671.x.
21. **Epstein JE, Tewari K, Lyke KE, Sim BK, Billingsley PF, Laurens MB, Gunasekera A, Chakravarty S, James ER, Sedegah M, Richman A, Velmurugan S, Reyes S, Li M, Tucker K, Ahumada A, Ruben AJ, Li T, Stafford R, Eappen AG, Tamminga C, Bennett JW, Ockenhouse CF, Murphy JR, Komisar J, Thomas N, Loyevsky M, Birkett A, Plowe CV, Loucq C, Edelman R, Richie TL, Seder RA, Hoffman SL.** 2011. Live attenuated malaria vaccine designed to protect through hepatic CD8$^+$ T cell immunity. Science **334:**475–480. http://dx.doi.org/10.1126/science.1211548.
22. **Imai T, Ishida H, Suzue K, Hirai M, Taniguchi T, Okada H, Suzuki T, Shimokawa C, Hisaeda H.** 2013. CD8$^+$ T cell activation by murine erythroblasts infected with malaria parasites. Sci Rep **3:**1572. http://dx.doi.org/10.1038/srep01572.
23. **Perkins DJ, Were T, Davenport GC, Kempaiah P, Hittner JB, Ong'echa JM.** 2011. Severe malarial anemia: innate immunity and pathogenesis. Int J Biol Sci **7:**1427–1442. http://dx.doi.org/10.7150/ijbs.7.1427.
24. **Waitumbi JN, Opollo MO, Muga RO, Misore AO, Stoute JA.** 2000. Red cell surface changes and erythrophagocytosis in children with severe Plasmodium falciparum anemia. Blood **95:**1481–1486. http://www.bloodjournal.org/content/bloodjournal/95/4/1481.full.pdf..
25. **Gwamaka M, Fried M, Domingo G, Duffy PE.** 2011. Early and extensive CD55 loss from red blood cells supports a causal role in malarial anaemia. Malar J **10:**386. http://dx.doi.org/10.1186/1475-2875-10-386.
26. **Zuckerman A.** 1957. Blood loss and replacement in plasmodial infections. I. Plasmodium berghei in untreated rats of varying age and in adult rats with erythropoietic mechanisms manipulated before inoculation. J Infect Dis **100:**172–206. http://dx.doi.org/10.1093/infdis/100.2.172.
27. **Spira D, Zuckerman A.** 1965. Blood loss and replacement in plasmodial infections. VI. Plasmodium berghei in splenectomized rats. J Infect Dis **115:**337–344. http://dx.doi.org/10.1093/infdis/115.4.337.
28. **Pierrot C, Adam E, Hot D, Lafitte S, Capron M, George JD, Khalife J.** 2007. Contribution of T cells and neutrophils in protection of young susceptible rats from fatal experimental malaria. J Immunol **178:**1713–1722. http://dx.doi.org/10.4049/jimmunol.178.3.1713.
29. **Lundie RJ, de Koning-Ward TF, Davey GM, Nie CQ, Hansen DS, Lau LS, Mintern JD, Belz GT, Schofield L, Carbone FR, Villadangos JA, Crabb BS, Heath WR.** 2008. Blood-stage plasmodium infection induces CD8$^+$ T lymphocytes to parasite-expressed antigens, largely regulated by CD8alpha$^+$ dendritic cells. Proc Natl Acad Sci U S A **105:**14509–14514. http://dx.doi.org/10.1073/pnas.0806727105.
30. **Miyakoda M, Kimura D, Yuda M, Chinzei Y, Shibata Y, Honma K, Yui K.** 2008. Malaria-specific and nonspecific activation of CD8$^+$ T cells during blood stage of Plasmodium berghei infection. J Immunol **181:**1420–1428. http://dx.doi.org/10.4049/jimmunol.181.2.1420.
31. **Amante FH, Haque A, Stanley AC, Rivera Fde L, Randall LM, Wilson YA, Yeo G, Pieper C, Crabb BS, de Koning-Ward TF, Lundie RJ, Good MF, Pinzon-Charry A, Pearson MS, Duke MG, McManus DP, Loukas A, Hill GR, Engwerda CR.** 2010. Immune-mediated mechanisms of parasite tissue sequestration during experimental cerebral malaria. J Immunol **185:**3632–3642. http://dx.doi.org/10.4049/jimmunol.1000944.
32. **Claser C, Malleret B, Gun SY, Wong AY, Chang ZW, Teo P, See PC, Howland SW, Ginhoux F, Rénia L.** 2011. CD8$^+$ T cells and IFN-γ mediate the time-dependent accumulation of infected red blood cells in deep organs during experimental cerebral malaria. PLoS One **6:**e18720. http://dx.doi.org/10.1371/journal.pone.0018720.
33. **Horne-Debets JM, Faleiro R, Karunarathne DS, Liu XQ, Lineburg KE, Poh CM, Grotenbreg GM, Hill GR, MacDonald KP, Good MF, Renia L, Ahmed R, Sharpe AH, Wykes MN.** 2013. PD-1 dependent exhaustion of CD8$^+$ T cells drives chronic malaria. Cell Rep **5:**1204–1213. http://dx.doi.org/10.1016/j.celrep.2013.11.002.
34. **Embury SH, Clark MR, Monroy G, Mohandas N.** 1984. Concurrent sickle cell anemia and alpha-thalassemia. Effect on pathological properties of sickle erythrocytes. J Clin Invest **73:**116–123. http://dx.doi.org/10.1172/JCI111181.
35. **Sedegah M, Sim BK, Mason C, Nutman T, Malik A, Roberts C, Johnson A, Ochola J, Koech D, Were B, Hoffman SL.** 1992. Naturally acquired CD8$^+$ cytotoxic T lymphocytes against the Plasmodium falciparum circumsporozoite protein. J Immunol **149:**966–971. http://www.jimmunol.org/content/149/3/966.long..
36. **Good MF, Doolan DL.** 2010. Malaria vaccine design: immunological considerations. Immunity **33:**555–566. http://dx.doi.org/10.1016/j.immuni.2010.10.005.
37. **Pombo DJ, Lawrence G, Hirunpetcharat C, Rzepczyk C, Bryden M, Cloonan N, Anderson K, Mahakunkijcharoen Y, Martin LB, Wilson D, Elliott S, Elliott S, Eisen DP, Weinberg JB, Saul A, Good MF.** 2002. Immunity to malaria after administration of ultra-low doses of red cells infected with Plasmodium falciparum. Lancet **360:**610–617. http://dx.doi.org/10.1016/S0140-6736(02)09784-2.
38. **Howland SW, Poh CM, Gun SY, Claser C, Malleret B, Shastri N, Ginhoux F, Grotenbreg GM, Rénia L.** 2013. Brain microvessel cross-presentation is a hallmark of experimental cerebral malaria. EMBO Mol Med **5:**916–931. http://dx.doi.org/10.1002/emmm.201202273.
39. **Martin-Jaular L, Nakayasu ES, Ferrer M, Almeida IC, Del Portillo HA.** 2011. Exosomes from plasmodium yoelii-infected reticulocytes protect mice from lethal infections. PLoS One **6:**e26588. http://dx.doi.org/10.1371/journal.pone.0026588.
40. **Jones TR, Stroncek DF, Gozalo AS, Obaldia N, III, Andersen EM, Lucas C, Narum DL, Magill AJ, Sim BK, Hoffman SL.** 2002. Anemia in parasite- and recombinant protein-immunized aotus monkeys infected with Plasmodium falciparum. Am J Trop Med Hyg **66:**672–679. http://www.ajtmh.org/content/66/6/672.long..

41. **Sagara I, Dicko A, Ellis RD, Fay MP, Diawara SI, Assadou MH, Sissoko MS, Kone M, Diallo AI, Saye R, Guindo MA, Kante O, Niambele MB, Miura K, Mullen GE, Pierce M, Martin LB, Dolo A, Diallo DA, Doumbo OK, Miller LH, Saul A.** 2009. A randomized controlled phase 2 trial of the blood stage AMA1-C1/Alhydrogel malaria vaccine in children in Mali. Vaccine **27:**3090–3098. http://dx.doi.org/10.1016/j.vaccine.2009.03.014.
42. **Ellis RD, Fay MP, Sagara I, Dicko A, Miura K, Guindo MA, Guindo A, Sissoko MS, Doumbo OK, Diallo D.** 2011. Anaemia in a phase 2 study of a blood stage falciparum malaria vaccine. Malar J **10:**13. http://dx.doi.org/10.1186/1475-2875-10-13.
43. **Janse CJ, Ramesar J, Waters AP.** 2006. High-efficiency transfection and drug selection of genetically transformed blood stages of the rodent malaria parasite Plasmodium berghei. Nat Protoc **1:**346–356. http://dx.doi.org/10.1038/nprot.2006.53.
44. **World Health Organization.** 2000. Severe falciparum malaria. World Health Organization, communicable diseases cluster. Trans R Soc Trop Med Hyg **94**(Suppl 1):S1–S90. http://whqlibdoc.who.int/publications/2000/TropMedandHygiene_2000_94_S1_pp1-10.pdf.
45. **Silamut K, Phu NH, Whitty C, Turner GD, Louwrier K, Mai NT, Simpson JA, Hien TT, White NJ.** 1999. A quantitative analysis of the microvascular sequestration of malaria parasites in the human brain. Am J Pathol **155:**395–410. http://dx.doi.org/10.1016/S0002-9440(10)65136-X.